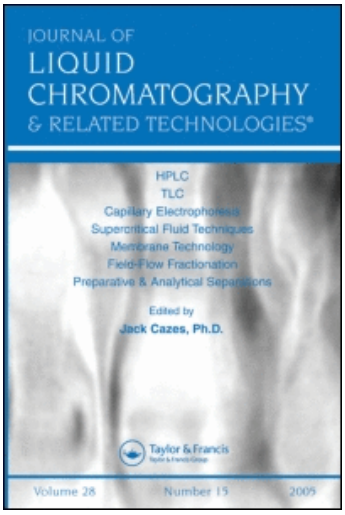

Journal of Liquid Chromatography & Related Technologies
Publication details, including instructions for authors and subscription information:
http://www.informaworld.com/smpp/title~content=t713597273

Nonequilibrium and Polydispersity Peak Broadening in Thermal Field-Flow Fractionation

Michel Martin[a]; Marcus N. Myers[a]; J. Calvin Giddings[a]
[a] Department of Chemistry, University of Utah, Salt Lake City, Utah

To cite this Article Martin, Michel , Myers, Marcus N. and Giddings, J. Calvin(1979) 'Nonequilibrium and Polydispersity Peak Broadening in Thermal Field-Flow Fractionation', Journal of Liquid Chromatography & Related Technologies, 2: 2, 147 — 164
To link to this Article: DOI: 10.1080/01483917908060055
URL: http://dx.doi.org/10.1080/01483917908060055

JOURNAL OF LIQUID CHROMATOGRAPHY, 2(2), 147-164 (1979)

NONEQUILIBRIUM AND POLYDISPERSITY PEAK BROADENING IN THERMAL FIELD-FLOW FRACTIONATION

Michel Martin, Marcus N. Myers, and J. Calvin Giddings
Department of Chemistry
University of Utah
Salt Lake City, Utah 84112

ABSTRACT

New theoretical procedures and an expanded data base have been combined to yield improved calculations for nonequilibrium plate height and polydispersity contributions in field-flow fractionation (FFF). Five thermal FFF column systems having a fourfold range in column width and length were operated with four solutes to yield eleven distinct channel-solute systems. After data were corrected for relaxation effects, comparison of experimental plate height measurements with theory showed good overall agreement for nonequilibrium parameter χ. Calculated values of polydispersity agreed reasonably well with supplier's values. Data reliability has been discussed in relationship to column dimensions and experimental parameters.

INTRODUCTION

In a previous paper considerable progress was reported toward the goal of isolating different plate height contributions in thermal field-flow fractionation (FFF) and assessing their relative importance (1). The principal peak broadening mechanism was found to originate in the nonequilibrium process, which is a fundamental phenomenon of great importance in all FFF subtechniques (2-4). However, there appeared to be measurable contributions from sample polydispersity and in some cases from relaxation phenomena as well. (Equations describing these

various contributions can be found in the cited paper (1).) Altogether, reasonable agreement was found between experimental trends and theoretical calculations.

In this study we expand on the previous work by employing a wider variety of column types in five individual channel systems rather than two. Whereas the two channels used in the previous work were identical in dimensions, the five channel systems of this study involve a fourfold range in both column width and length, the two critical dimensional parameters of FFF channels. These additions provide not only an expanded opportunity to compare theory and experiment, but also the opportunity to determine whether any trends develop with changes in these two dimensions outside the predictions of theory.

Furthermore, we have developed procedures to calculate more accurate plate height parameters based on recent refinements in theory. The most notable improvements are in the treatment of the nonequilibrium contributions.

In summary, we have focused both new experimental and improved theoretical efforts on the limited goal of isolating and measuring nonequilibrium and polydispersity contributions to the plate height of thermal FFF columns.

THEORY

Diverse plate height contributions in FFF were summarized in the previous paper (1). Of these contributions, we are particularly interested in the nonequilibrium component

$$H_N = \chi w^2 \langle v \rangle / D \tag{1}$$

and the polydispersity contribution

$$H_p = L \left(\frac{d \ln V_r}{d \ln M} \right)^2 \frac{\mu - 1}{\mu} \tag{2}$$

In these equations w is the channel width, $\langle v \rangle$ the velocity, D the diffusion coefficient, L the channel length, V_r the retention

volume, M the molecular weight, and μ the polydispersity, which is equal to $\bar{M}_w/\bar{M}_n$. Coefficient χ is a complicated term whose nature we shall discuss shortly. This coefficient and all the retention parameters such as V_r are functions of a dimensionless parameter λ which approximately represents the ratio of the mean thickness of the solute layer to channel width w (see Eqn. 12). The fundamental expression for λ is

$$\lambda = D/Uw \tag{3}$$

where U is the average velocity of the solute induced by the existence of a field or gradient perpendicular to flow. For common parabolic flow profiles in the channel, retention ratio R (void volume/retention volume) is given by the equation

$$R = 6\lambda \left[\coth(1/2\lambda) - 2\lambda\right] \tag{4}$$

Under circumstances in which all other contributions are negligible and the measured plate height H_{app} can be represented by the sum of $H_N + H_p$, Eqns. 1 and 2 yield the following expression

$$H_{app} = H_N + H_p = \frac{\chi w^2}{D} \langle v \rangle + L \left(\frac{d \ln V_r}{d \ln M}\right)^2 \frac{\mu - 1}{\mu} \tag{5}$$

For this case it is seen that a plot of H_{app} versus flow velocity $\langle v \rangle$ yields a straight line whose slope depends on nonequilibrium parameter χ and whose intercept is a function of polydispersity μ. Specifically we have

$$\text{slope} = \chi w^2/D \tag{6}$$

and

$$\text{intercept} = L \left(\frac{d \ln V_r}{d \ln M}\right)^2 \frac{\mu - 1}{\mu} \tag{7}$$

The above two equations permit us to make quantitative comparisons between theoretical and experimental nonequilibrium and polydispersity parameters.

While we assume here that nonequilibrium and polydispersity dominate the plate height expression as indicated by Eqn. 5, we also note that the relaxation contribution is sometimes important and that a correction for relaxation may improve the reliability of the data. In order to make the relaxation correction we employ the following equation for its plate height contribution (1)

$$H_r = \frac{17}{140} \frac{n}{L} \left(\frac{w^2 \langle v \rangle \lambda}{D} \right)^2 \qquad (8)$$

where n, the effective number of relaxation processes in the column, has been assumed equal to unity. Values calculated according to Eqn. 8 are simply subtracted from H_{app} to yield corrected plate heights. All data in this paper have been so corrected unless otherwise noted.

Below we discuss improved methods for calculating χ and μ.

METHOD FOR DETERMINATION OF χ AND μ

In order to determine the nonequilibrium coefficient χ from the slope of the plate height versus velocity curve according to Eqns. 5 and 6, the thickness of the channel, w, and the diffusion coefficient of the solute, D, must be known. We have used the nominal value of the Mylar spacer thickness given by the manufacturer for w. The diffusion coefficient, expressed in cm^2/sec, was evaluated by a formula established in a previous study (5)

$$D = M^A \exp\left(B + \frac{C}{T}\right) \qquad (9)$$

where T is temperature in ^oK and A, B, and C are empirical coefficients which for polystyrenes in ethylbenzene have been found equal to A = -0.552, B = -3.6851, C = -1360.

For precise calculations, the temperature T in Eqn. 9--along with other parameters that vary across the channel--should be taken at the position of the center of gravity of the solute zone, a distance x_{cg} above the cold wall (6). The temper-

ature at this point, T_{cg}, is closely approximated by (5)

$$T_{cg} = T_C + \Delta T \frac{-a + \sqrt{a^2+4(1-a)x_{cg}/w}}{2(1-a)} \quad (10)$$

where T_c is the temperature at the cold wall, ΔT the temperature drop across the channel and a is equal to

$$a = 1/[1 + (dk/dt)\Delta T/2k_c] \quad (11)$$

where k is the thermal conductivity of the eluent and k_c is its value at the cold wall temperature. Eqns. 10 and 11 are based on the assumption that the thermal conductivity of the solvent is a linear function of temperature, thus giving the parabolic relationship expressed in Eqn. 10 (5). For ethylbenzene at 293°K, $(1/2\ k_c)(dk/dT) = -9.22 \times 10^{-4}\ {}^{o}K^{-1}$ (7). The temperature profile, $(T - T_c)/\Delta T = \delta T/\Delta T$ versus x/w, is given in Fig. 1 for ethylbenzene with $T_c = 293^{o}K$. Center of gravity values can be found by replacing T by T_{cg} and x by x_{cg}. The center of gravity position, x_{cg}, for use in Eqn. 10, is obtained from λ by the equation (6)

$$x_{cg}/w = \lambda - e^{-1/\lambda}/(1-e^{-1/\lambda}) \quad (12)$$

A plot of x_{cg}/w versus λ is shown in Fig. 2. It is seen that values of x_{cg}/w rapidly approach λ as λ approaches zero. Thus when λ is smaller than 0.18 (that is, $R < 0.7$ in Eqn. 4) x_{cg}/w can be equated to λ with an error of less than 0.4%.

Quantity λ is obtained from the experimental retention ratio R. While Eqn. 4 is generally used for this purpose in FFF, this equation is only approximately valid for solute zones in thermal FFF. The inexactness of Eqn. 4 stems from the temperature dependence of the solvent viscosity which leads to a nonparabolic flow profile in thermal FFF. It has been shown that a simple third degree equation can be used to a very good approximation for the complicated expression describing this phenomenon (8). The relationship between R and λ is then given by

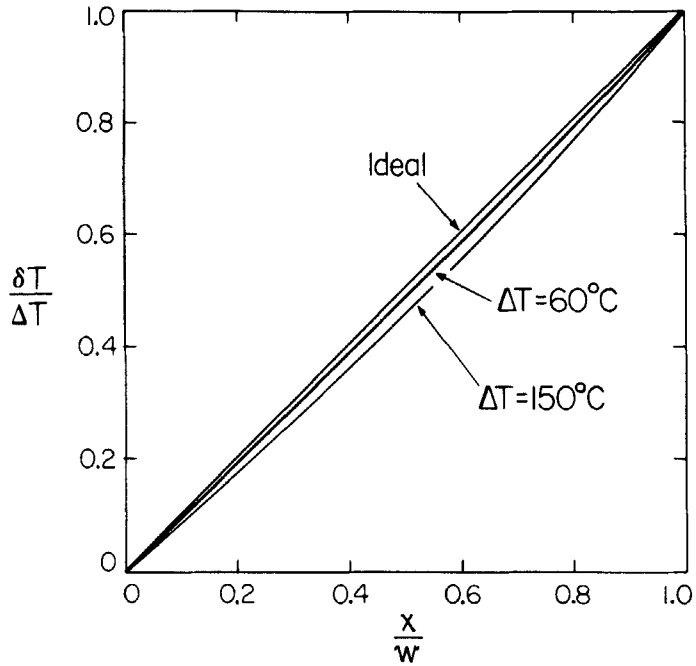

FIGURE 1. Temperature profile in thermal FFF channel for ethylbenzene at 293°K, cold wall. Quantity δT is temperature elevation above cold wall temperature while x/w is fractional distance across channel. Total temperature drop is ΔT.

$$R = 6\lambda\nu(1-R_p) + R_p \qquad (13)$$

where R_p is the retention ratio corresponding to a parabolic flow and given by Eqn. 4, and ν is a third-order adjustment parameter for the distortion of the flow, the magnitude of which depends on the nature of the solvent and on the temperature profile in the channel (8). In this paper Eqn. 13 is used to obtain the fundamental parameter λ from experimental measurements of R, where ν is taken from the curves in reference (8).

In summary, values of λ obtained using Eqn. 13 allow us to determine x_{cg}/w from Eqn. 12, and subsequently T_{cg} from Eqns. 10 and 11 and D from Eqn. 9. With these parameters and a value for

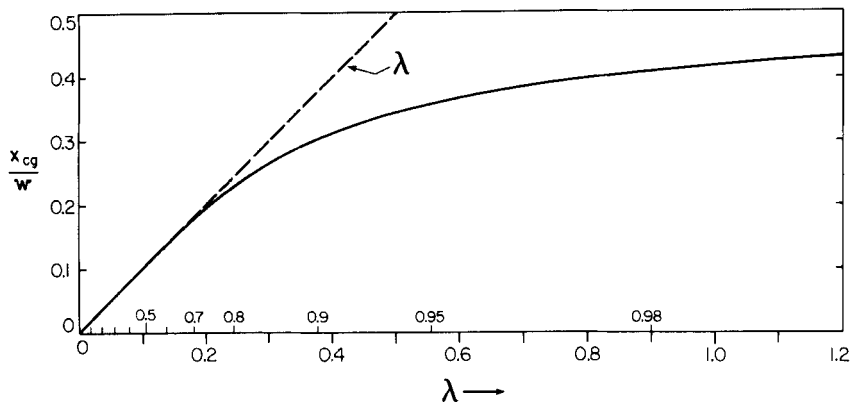

FIGURE 2. Plot of x_{cg}/w versus λ for exponential solute layers.

w, it is possible to obtain experimental values of χ from the measured slope of the plate height versus velocity curve using Eqn. 6. These values can be compared to theoretical χ's using a complicated expressing of λ and ν appearing as Eqns. 25, 59, 60, 67, 68, and 69 in another paper (9). The polydispersity, μ, of polymer samples is obtained from the intercept of the plate height curve as shown by Eqn. 7. The term $d \ln V_r / d \ln M$ can be obtained from an empirical calibration curve or, indirectly, from λ and ν since $(d\ln V_r/d\ln M)^2 = (d\ln R/d\ln\lambda)^2 (d\ln\lambda/d\ln M)^2 = \gamma^2 (d\ln R/d\ln\lambda)^2$. The parameter $\gamma = |d\ln\lambda/d\ln M|$, and is found empirically to lie in the range 0.5-0.6 (10). In this paper we use $\gamma = 0.55$. The value of $d\ln R/d\ln\lambda$ is obtained from Eqns. 13 and 4.

$$\frac{d \ln R}{d \ln} = 1 - \frac{6\nu\lambda R_p}{R} + \frac{12\lambda(1-6\lambda\nu)}{R} \left\{ \frac{\exp(-1/\lambda)}{\lambda[1-\exp(1/\lambda)]} 2^{-\lambda} \right\} \quad (14)$$

EXPERIMENTAL

The physical characteristics of the five channel systems used in this study are shown in Table 1. The first four systems have been previously described (10). In each case the channel is cut

in a Mylar sheet which is clamped between two metal bars. The channels are tapered at their extremities and at the position of each apex a hole drilled in the top bar provides for inlet and outlet of eluent and sample.

Channel V is a unique new "hairpin" channel consisting of four parallel paths cut from a wide Mylar sheet and joined at their ends by narrow ($\sim$ 1 mm) curving pathways. This configuration allows an increase by a factor of four in the length of the separation channel without an increase in the apparatus length.

With this system, two very similar channels were built with the same spacer thickness (w = 0.127 mm). They are labeled Va and Vb in Table 1, and were found to give nearly identical results.

The construction details and separative performance of channels Va and Vb will be presented in another paper (11).

All samples were injected by a Microliter #701 syringe and monitored by a Waters R401 RI detector. The procedural details have been presented elsewhere (10,12).

The 51,000 MW polystyrene polymer sample was obtained from Mann Research Laboratories, the 110,000 MW sample from Pressure Chemical Company, and the 160,000 MW sample from Waters Associates. The polydispersity values, $\mu = \bar{M}_w/\bar{M}_n$, provided

TABLE 1

Characteristics of the Thermal FFF Channel used in this Study

Channel Number	Channel Surface	Length L (mm)	Thickness w (mm)	Breadth a (mm)	Volume V^o (ml)
I	Au	433	0.254	20	2.20
II	Au	414	0.127	20	1.05
III	Cu	427	0.127	20	1.08
IV	Cu	423	0.0508	20	0.43
Va	Cr	1802	0.127	10	2.29
Vb	Cr	1844	0.127	10	2.34

by the suppliers, were $\mu < 1.06$ for the Mann and Pressure Chemical samples, and $\mu < 1.009$ for the Waters material.

RESULTS AND DISCUSSION

Plate height data have been obtained for eleven distinct solute-channel systems by performing from 11 to 20 experimental runs per system. The operating conditions, channels, polymer molecular weights and sources, along with calculated values of ν and D are summarized in Table 2. Experimental values of retention ratio R and various derivative parameters of importance are summarized for the eleven systems in Table 3.

TABLE 2

Operating Conditions and Parameters for the Eleven Systems Studied in this Paper. Solutes, with One Indicated Exception, are Linear Polystyrene Polymers of the Specified Molecular Weights.

System Number	Channel Number	w (mm)	Solute Mol. Wt.	ΔT (°C)	T_c (°C)	ν	D x 10^7 (cm^2/sec)
1	I (Au)	0.254	110,000 (PCC)	60	20	-0.204	4.24
2	I (Au)	0.254	51,000 (Mann)	60	20	-0.204	6.76
3	II (Au)	0.127	110,000 (PCC)	60	20	-0.204	4.26
4	II (Au)	0.127	51,000 (Mann)	60	20	-0.204	6.83
5	II (Au)	0.127	nC_7H_{16}	0	25	0	182
6	III (Cu)	0.127	51,000 (Mann)	60	21	-0.202	6.92
7	III (Cu)	0.127	160,000 (Wat)	60	21	-0.202	3.48
8	IV (Cu)	0.051	51,000 (Mann)	56	35	-0.177	8.63
9	IV (Cu)	0.051	160,000 (Wat)	56	35	-0.177	4.34
10	Va (Cr)	0.127	160,000 (Wat)	60	23	-0.200	3.59
11	Vb (Cr)	0.127	51,000 (Wat)	60.1	23.3	-0.200	7.16

PCC = Pressure Chemical Company polymer ($\mu < 1.06$)

Mann = Mann Research Laboratories polymer ($\mu < 1.06$)

Wat = Waters Associates polymer ($\mu < 1.0009$)

TABLE 3

Experimental Retention Ratio R and Derivative Parameters which Bear on Solute Migration and Plate Height.

System Number	R	λ	d ln R/d ln λ	x_{cg}/w	T_{cg}
1	0.31	0.070	0.894	0.070	24.0
2	0.47	0.116	0.733	0.116	26.6
3	0.32	0.073	0.885	0.073	24.2
4	0.51	0.130	0.734	0.129	27.4
5	1	∞	-	0.500	25
6	0.50	0.126	0.743	0.126	28.2
7	0.27	0.061	0.911	0.061	24.5
8	0.61	0.165	0.616	0.163	43.7
9	0.37	0.085	0.850	0.085	39.5
10	0.27	0.061	0.911	0.061	26.5
11	0.50	0.126	0.744	0.126	30.5

Plate height plots were made for these eleven systems using both raw plate height data and data corrected for relaxation. Figure 3 shows plots for two of the channel systems as least squares straight lines which have been fit to the data. The raw data are also shown. This figure shows that system #1 is subject to a very large relaxation correction, whereas the correction for system #4 is relatively small. This is consistent with Eqn. 8 which shows that the relaxation contribution is proportional to w^4. Systems #1 and #2--having the largest width, w, of any of the solute-channel systems--are therefore expected to exhibit the biggest corrections for relaxation.

We note that the uncorrected lines in Fig. 3 tend to intercept the H axis at a point lower than the corrected lines. This arises in the nature of the relaxation correction. The divergence in intercepts between corrected and uncorrected plots is

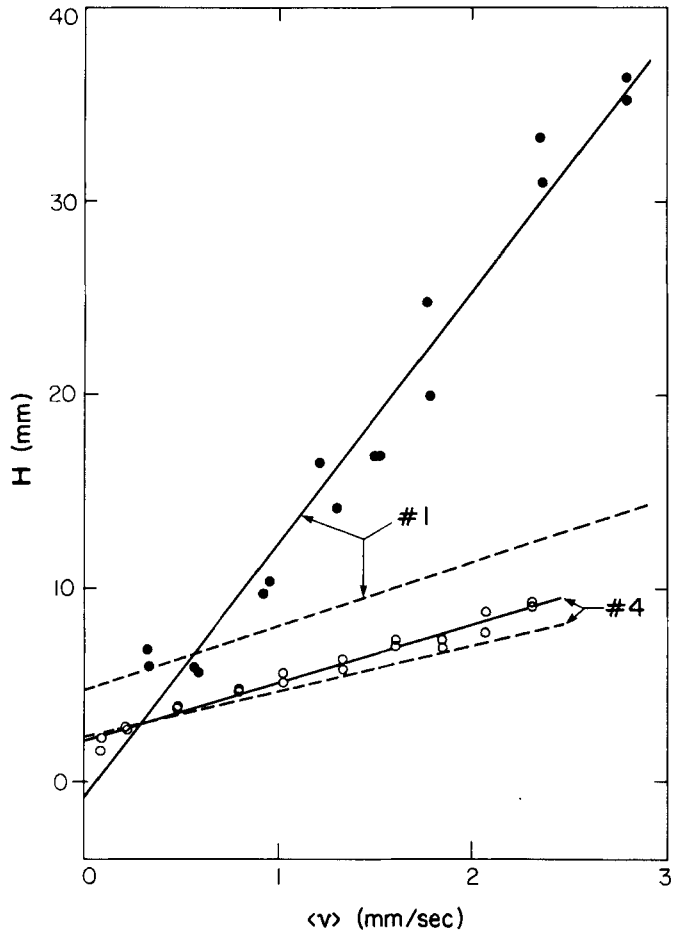

FIGURE 3. Plate height plots for system #'s 1 and 4. Solid lines are fit by least squares to the raw data (shown in the figure) while dashed lines are fit to data corrected for relaxation.

therefore expected to increase with the magnitude of the correction. This divergence is so large for system #1 that the uncorrected curve shows a negative intercept, as illustrated in the figure. Because the corrected plots must be regarded as the more

reliable of the two sets, all the remaining data and plots in this paper are reported for the corrected data only.

Figure 4 shows the corrected straight line plots for ten systems (excluding the nonretained system, #5). The slopes of these plots yield the nonequilibrium χ parameters as shown by Eqn. 6. Both experimental and theoretical χ values calculated by the procedures outlined earlier in this paper are shown in the left hand part of Table 4.

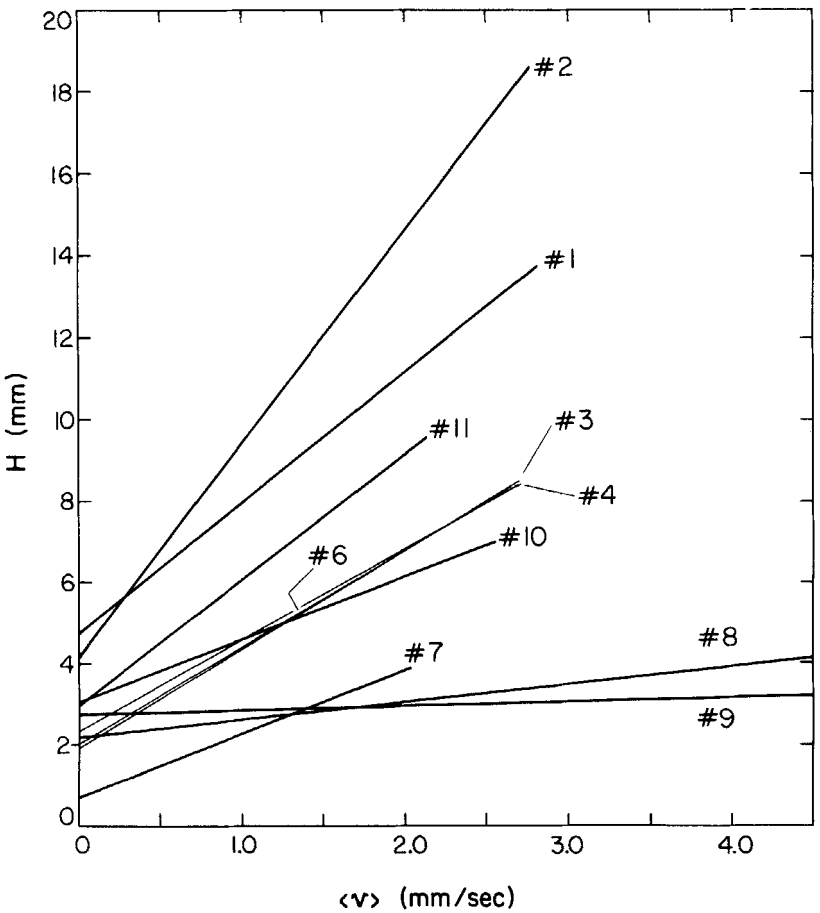

FIGURE 4. Least squares plate height plots for ten systems. All experimental data were corrected for relaxation.

TABLE 4

System Number	Slope (sec)	χ_{exp} x10^3	χ_{theor} x10^3	$\frac{\chi_{exp}-\chi_{theor}}{\chi_{theor}} \times 100$	Intercept (mm)	μ
1	3.19	2.10	4.18	-49.7	4.74	1.047
2	5.22	5.47	1.19	-54.0	4.15	1.056
3	2.41	6.37	4.74	+34.3	1.92	1.020
4	2.24	9.50	14.0	-32.0	2.31	1.035
5	0.087	9.82	9.52	+ 3.1	0.17	-
6	2.38	10.2	13.4	-23.8	2.00	1.029
7	1.56	3.36	2.99	+12.6	0.68	1.006
8	0.44	1.46	17.8	-18.2	2.16	1.047
9	0.10	1.62	6.46	-74.9	2.76	1.031
10	1.54	3.43	2.97	+15.5	3.03	1.007
11	3.08	13.1	13.4	+ 2.2	2.95	1.010

The highly variable slopes of the lines in Fig. 4 can be qualitatively understood, although the interpretation is somewhat complicated by the fact that two parameters are here acting independently to establish these slopes. First, according to Eqn. 6, the slope increases sharply with channel width w. Second, it can be shown that χ increases rapidly with decreasing molecular weight, so that the slope increases rapidly as molecular weight declines. In view of these trends, it is not surprising that the highest slope in Fig. 4 is for system #2, which utilizes both the thickest channel (w = 0.254 mm) and the lowest polymer molecular weight (51,000). The lowest slope, on the other hand, is for system #9 which is based on an ultrathin channel system (w = 0.051 mm) and the polymer of highest molecular weight (160,000). The lines between these extremes follow the same trends for the most part, but there are some exceptions which probably result from experimental inaccuracies.

The comparison of χ values derived from the slopes in Fig. 4 with theoretical values sheds more light on the level of experimental reliability. The entries of Table 4 show good overall agreement between theory and experiment, considering the previous difficulties encountered in such measurements (1). The average absolute value of the deviation of χ_{exp} from χ_{theor} is only about 29 percent, although, as shown in Table 4, the χ_{exp} values for channel no. 1 (system #'s 1 and 2) are consistently only about half of the theoretical values. It appears in these cases almost as if the relaxation correction were too large, although no immediate explanation for this is apparent. The ultrathin channel, too, gives poor agreement in system #9, but this can be attributed to the difficulties of measuring a slope that is exceedingly small to begin with. Clearly, the thinner channels in general yield more consistent values: if we exclude systems #1 and #2 the average absolute deviation from theoretical reduces from 29 percent to 24 percent, and if we leave out system #9 this drops to 18 percent, a commendable value by present standards.

The most reliable channel is undoubtedly number V, used in systems #10 and #11. The small average absolute deviation for these systems, 9 percent, is expected because of the greater length (1.8 m) of the channel and the minimization of relaxation effects and end effects in general.

The intercepts of the lines with the H axis in Fig. 4 are also shown in Table 4. Values of polydispersity, μ, were calculated from Eqn. 7 and the procedures outlined for obtaining $d \ln V_r / d \ln M$. The μ values are also reported in Table 4. While precise independent values for polydispersity are not known, the companies supplying these polymers have established some limits which help us judge the reliability of the derived polydispersity data. As noted earlier, Mann Research Laboratories and Pressure Chemical Company both indicate that μ values are less than 1.06. The maximum value of μ for the Waters Associates polymers is stated to be 1.009. While the μ values of Table 4 show rough

agreement with these numbers, there is considerable scatter which may have its origin either in the experimental measurements or in the polymer samples themselves.

In order to attempt to establish some pattern for polydispersity, plate height lines are plotted in Fig. 5 in the form 5 H/L, which, from Eqn. 2, is seen to be more directly related to polydispersity than is H. The number 5 is approximately the

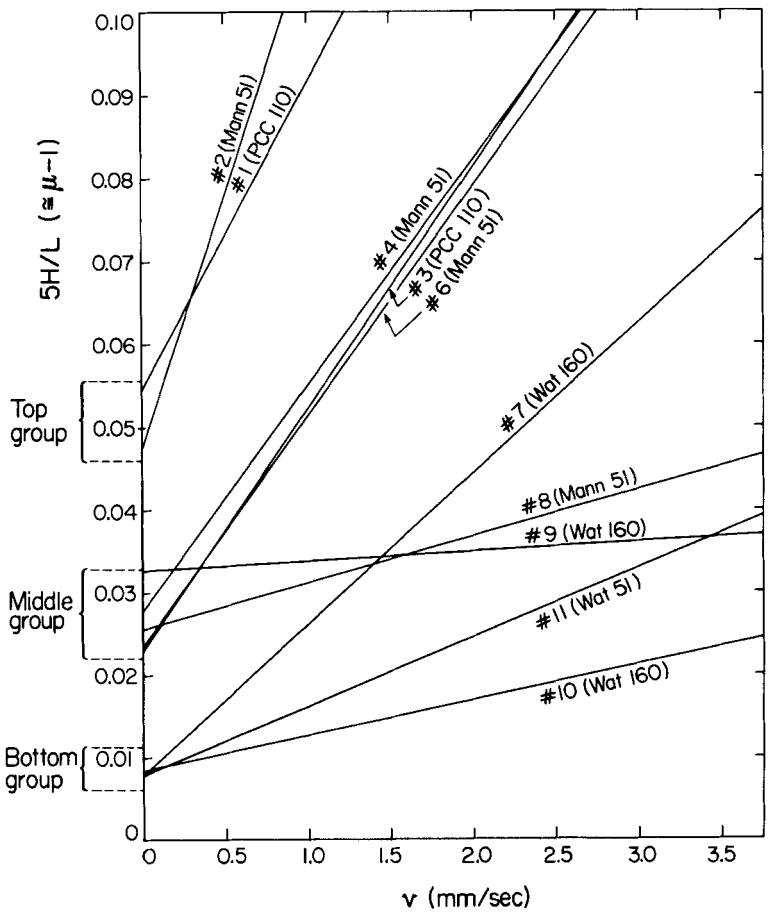

FIGURE 5. Plots of 5H/L, whose intercepts correspond roughly to μ-1.

reciprocal of the average value of the square of $d \ln V_r / d \ln M$ for the various systems. (For high retention levels, a better number is 3.3.) Thus, to a rough approximation, the intercept represents the quantity $(\mu-1)/\mu$; as confirmed by Eqn. 5. In that μ is approximately unity for the polymers employed in this work, the intercept very nearly represents the quantity $\mu-1$. (Exact correspondence of the intercepts with the μ values in Table 4 cannot be expected because of the approximations.)

The intercepts of Fig. 5 fall into three rather distinct groups as indicated on the left hand border. In order to help clarify our analysis of these groups, we have labeled each plot with the system number from which it is derived, the polymer supplier, and the polymer molecular weight measured in thousands.

Figure 5 shows that the intercepts of the two lines of the top group fall into a narrow range around 0.05, corresponding to a μ value of 1.05. Both of these intercepts occur for polymers which are specified to have $\mu < 1.06$. Thus the agreement is rather close. Likewise with the bottom group, the intercepts cluster tightly around 0.008, corresponding to $\mu = 1.008$, which is in excellent accord with the upper limit of μ, 1.009, specified by the manufacturer for these polymer samples.

The middle group of intercepts in Figure 5 is, at least on the surface, more difficult to explain. These intercepts cluster in the general vicinity of 0.03, corresponding to $\mu = 1.03$. Unfortunately, there is no evidence indicating that any of the polymers have μ values in this vicinity. Furthermore, directly contradictory results can be found for the three polymers included in this group because each of them is located on at least one occasion in either the top group or the bottom group. It is possible that some significant experimental errors exist in these intercepts. This would not be surprising considering the difficulty of extrapolating data over a considerable span to obtain intercepts. Unfortunately, there are no independent data of any consequence to determine the correct values.

We note a few additional circumstances which may bear on the significance of the intercepts shown in Fig. 5. First of all, systems #8 and #9 were run with the ultrathin channel system ($w = 0.051$ mm) which is more prone to dead volume errors than the other channel systems. Hence some error in these intercepts would not be surprising. Furthermore the Waters 160,000 polystyrene used in system #9 should fall near or below the maximum value of $\mu = 1.009$ rather than at the substantially larger value of 1.033. While these considerations may discredit part of the intercept data of the middle group, we note that three separate channel systems in this group yield values close to 1.026 for the Mann 51,000 polystyrene. While this agreement may be fortuitous, it certainly opens for consideration the possibility that the polydispersity in this particular polymer is closer to 1.026 than it is to 1.06. In fact, the large relaxation correction incurred for system #1 and #2 make the $\sim$ 1.05 intercepts more suspect than the $\sim$ 1.03 intercepts obtained with more reliable systems.

While some significant errors in the experimental determination of both χ and μ are evident in the results of this paper, we note that the results on the whole are in good agreement with independently derived data. Nonetheless, it should be the object of future work to further erode the errors and uncertainties in experimental values. When this is done one would certainly have, among other things, a useful tool for independently measuring the polydispersity of narrow cut polymer samples. We note that the intrinsic resolution of FFF is so high that only a few hundred plates have been necessary in most of the measurements that have led to experimental μ values.

While all the sources of error in peak broadening data are presently unclear, several improvements can be expected to have a beneficial effect on data reliability, First, it is likely that the use of more sensitive detectors with smaller injected samples would improve the quality of the data. Second, for channels of substantial thickness such as those used in system #1 and #2,

it would be helpful to use stop flow procedures (10,13) so that large relaxation corrections would not be necessary. These improvements coupled with a large number of runs (which could be more reliably interpreted by digital equipment) would undoubtedly yield more accurate data and provide greatly improved values for the fundamental parameters χ and μ.

ACKNOWLEDGMENT

This research was supported by National Science Foundation Grant No. CHE76-20870.

REFERENCES

1. Smith, L. K., Myers, M. N., and Giddings, J. C., Anal. Chem., 49, 1750, 1977.

2. Giddings, J. C., J. Chem. Phys., 49, 1, 1968.

3. Giddings, J. C., J. Chem. Ed., 50, 668, 1973.

4. Giddings, J. C., Yoon, Y. H., Caldwell, K. D., Myers, M. N., and Hovingh, M. E., Sep. Sci., 10, 447, 1975.

5. Giddings, J. C., Caldwell, K. D., and Myers, M. N., Macro-Molecules, 9, 106, 1976.

6. Hovingh, M. E., Thompson, G. H., and Giddings, J. C., Anal. Chem., 42, 1975, 1970.

7. Reid, R. C., and Sherwood, T. K., "The Properties of Gases and Liquids," 2nd Ed., McGraw-Hill, New York, 1966, p. 501.

8. Caldwell, K. D., Martin, M., and Giddings, J. C., Sep. Sci. & Tech., to be published.

9. Martin, M., and Giddings, J. C., J. Phys. Chem., submitted.

10. Myers, M. N., Caldwell, K. D., and Giddings, J. C., Sep. Sci., 9, 47, 1974.

11. Giddings, J. C., Martin, M., and Myers, M. N., to be submitted to Anal. Chem.

12. Giddings, J. C., Martin, M., and Myers, M. N. J. Chromatogr., 158, 419, 1978.

13. Yang, F. J., Myers, M. N., and Giddings, J. C., Anal. Chem., 49, 659, 1977.